Rydberg-interaction gates via adiabatic passage and phase control of driving fields

Huaizhi Wu, Xi-Rong Huang, Chang-Sheng Hu, Zhen-Biao Yang, and Shi-Biao Zheng
Fujian Key Laboratory of Quantum Information and Quantum Optics and Department of Physics, Fuzhou University, Fuzhou 350116, People's Republic of China
(Received 3 June 2017; published 23 August 2017)

In this paper we propose two theoretical schemes for implementation of quantum phase gates by engineering the phase-sensitive dark state of two atoms subjected to Rydberg-Rydberg interaction. Combining the conventional adiabatic techniques and currently developed approaches of phase control, a feasible proposal for implementation of a geometric phase gate is presented, where the conditional phase shift (Berry phase) is achieved by adiabatically and cyclically changing the parameters of the driving fields. Here we find that the geometric phase acquired is related to the way how the relative phase is modulated. In the second scheme, the system Hamiltonian is adiabatically changed in a noncyclic manner, so that the acquired conditional phase is not a Berry phase. A detailed analysis of the experimental feasibility and the effect of decoherence is also given. The proposed schemes provide new perspectives for adiabatic manipulation of interacting Rydberg systems with tailored phase modulation.

DOI: 10.1103/PhysRevA.96.022321

I. INTRODUCTION

Neutral atoms in highly excited and long-lived Rydberg states are considered the ideal architecture for quantum information processing since it provides strongly interatomic interaction on demand, while it keeps interacting with the environment weakly [1,2]. There have been numerous proposals to use Rydberg-Rydberg interactions for implementation of quantum logic gates [3–9], quantum error correction [10,11], quantum algorithms [12–14], and quantum repeaters [15–18]. By following the pioneering works proposed by Jaksch *et al.* [19] and Lukin *et al.* [20], promising schemes for realizing two-qubit controlled-Z and controlled-NOT gates that rely on dynamical control of dipolar coupling and intrinsic Förster interaction have been widely studied in both the Rydberg blockade [5,21–24] and antiblockade regimes [25,26]. Therein, the validity of the gate operations is predominantly determined by the detailed laser parameters as well as the Rydberg interaction strength. Experimental demonstrations in producing quantum entanglement of few Rydberg atoms [27,28] and two-qubit logic operations [24] have recently made great progress by addressing the system's evolutional dynamics; however, the fidelity achieved to date is significantly limited by the imprecise control of experimental parameters.

The requirement of precise control of coherent dynamics can be avoided by using the adiabatic techniques, such as stimulated Raman adiabatic passage (STIRAP) and adiabatic rapid passage (ARP), where the sensitivity to imprecise Rabi control and other experimental perturbations is strongly suppressed [29]. The theoretical proposals based on the STIRAP and the ARP have been proposed for coherent population transfer [30–34], preparation of entangled states [14,35], and implementation of quantum logic gates [7,8,36,37] with Rydberg atoms, which exhibit robustness properties against moderate fluctuations of experimental parameters. Furthermore, the adiabatic technique alternatively provides a chance for geometric manipulation of Rydberg systems [35,37,38], which is naturally robust against certain control errors [39,40] and is a promising approach for implementation of a built-in fault-tolerant two-qubit logic gate.

Here we put forward two schemes for implementing quantum phase gates via adiabatic passage and phase control of the driving fields. The first scheme is based on the geometric manipulation of the system's Hamiltonian in the parameter space. In contrast to the previously similar approach [35], the geometric phase acquired here is not due to the variance of the phase difference of the control pulses, and is alternatively accumulated by changing the phases of the driving fields in step and keeping the phase difference null. Remarkably, we find that the geometric phase acquired is strongly dependent on the way the relative phase is modulated. In the second scheme, the conditional phase shift is not of dynamical origin as well since the qubit system evolves in the dark state space, nor is it a Berry adiabatic phase as the system Hamiltonian is not cyclically changed. The conditional phase arises from the adiabatic manipulation of the dark state with staircase phase control. The experimental feasibility, gate fidelity, and docoherence effect for the proposed schemes are carefully studied.

This paper is organized as follows. In Sec. II we propose the level addressing scheme for two neutral atoms interacting via the Rydberg-Rydberg interaction and examine the role of the phases of driving fields in adiabatic control. In Sec. III the schemes for implementing conditional phase gates based on Berry phase and non-Berry adiabatic phase are presented. In Sec. IV we provide a detailed discussion about the experimental feasibility of the two schemes. In Sec. V the effect of atomic spontaneous emission and interatomic force on the gate fidelity is studied. The conclusion is given in Sec. VI.

II. DARK STATE OF TWO INTERACTING RYDBERG ATOMS

We first introduce the schematic description of the system. Consider a pair of identical three-level atoms with a ground state $|1\rangle$, an intermediate state $|2\rangle$, and a highly excited Rydberg state $|3\rangle$ [see Fig. 1(a)] which are trapped in optical tweezers or optical lattices. Two excitation lasers of optical frequencies resonantly drive the atomic transitions $|1\rangle \leftrightarrow |2\rangle$

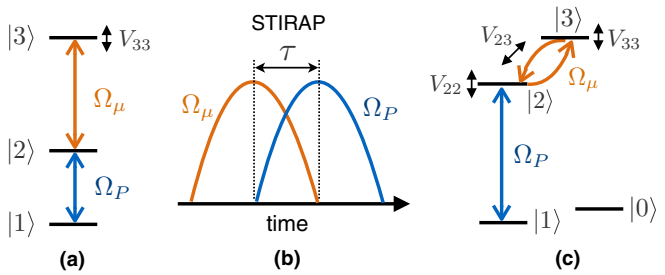

FIG. 1. (a) Schematic level configuration. The Rydberg state $|3\rangle$ is excited from the ground state $|1\rangle$ via an intermediate state $|2\rangle$ with two lasers of optical frequencies. Double excitation of the Rydberg state $|3\rangle$ will be shifted by V_{33} due to the interatomic interaction. Ω_p and Ω_μ are Rabi frequencies for the transitions $|1\rangle \leftrightarrow |2\rangle$ and $|2\rangle \leftrightarrow |3\rangle$, respectively. (b) STIRAP pulse sequence applied to the interacting Rydberg atoms with τ being the overlapping time. (c) Addressing scheme with multiple Rydberg levels. The ground state $|1\rangle$ is resonantly coupled to the Rydberg state $|2\rangle$ via single-photon transition with Rabi frequency Ω_p, and the atomic transition between Rydberg states $|2\rangle$ and $|3\rangle$ is driven by a microwave field with Rabi frequency Ω_μ. The ground state $|0\rangle$ is the auxiliary qubit state. V_{22}, V_{23}, and V_{33} are energy shifts induced by the Rydberg-Rydberg interaction.

and $|2\rangle \leftrightarrow |3\rangle$ with the Rabi frequencies $\Omega_p \equiv |\Omega_p|e^{i\phi_p}$ and $\Omega_\mu \equiv |\Omega_\mu|e^{-i\phi_\mu}$ (taken as a complex number), respectively. The atoms experience an energy shift V_{33} when both atoms are excited to the Rydberg state $|3\rangle$. The total Hamiltonian of the system in the rotating wave approximation is

$$\mathcal{H}_R = \mathcal{H}_1 \otimes \mathcal{I}_2 + \mathcal{I}_1 \otimes \mathcal{H}_2 + V_{33}|3\rangle_1|3\rangle_{22}\langle 3|_1\langle 3|, \quad (1)$$

with (from now on, we put $\hbar = 1$)

$$\mathcal{H}_i = \Omega_p|2\rangle_{ii}\langle 1| + \Omega_\mu|3\rangle_{ii}\langle 2| + \text{H.c.}, \quad i = 1,2. \quad (2)$$

In terms of the symmetric two-atomic basis states spanned by $\{|\phi_j\rangle\}$, $j = 1,\ldots,6$, with

$$\begin{aligned}
|\phi_1\rangle &= |1\rangle_1|1\rangle_2,\\
|\phi_2\rangle &= \frac{1}{\sqrt{2}}(|1\rangle_1|2\rangle_2 + |2\rangle_1|1\rangle_2),\\
|\phi_3\rangle &= \frac{1}{\sqrt{2}}(|1\rangle_1|3\rangle_2 + |3\rangle_1|1\rangle_2),\\
|\phi_4\rangle &= |2\rangle_1|2\rangle_2,\\
|\phi_5\rangle &= \frac{1}{\sqrt{2}}(|2\rangle_1|3\rangle_2 + |3\rangle_1|2\rangle_2),\\
|\phi_6\rangle &= |3\rangle_1|3\rangle_2,
\end{aligned}$$

$\mathcal{H}_R$ can be rewritten as

$$\mathcal{H}_R = \begin{bmatrix}
0 & \sqrt{2}\Omega_p^* & 0 & 0 & 0 & 0\\
\sqrt{2}\Omega_p & 0 & \Omega_\mu^* & \sqrt{2}\Omega_p^* & 0 & 0\\
0 & \Omega_\mu & 0 & 0 & \Omega_p^* & 0\\
0 & \sqrt{2}\Omega_p & 0 & 0 & \sqrt{2}\Omega_\mu^* & 0\\
0 & 0 & \Omega_p & \sqrt{2}\Omega_\mu & 0 & \sqrt{2}\Omega_\mu^*\\
0 & 0 & 0 & 0 & \sqrt{2}\Omega_\mu & V_{33}
\end{bmatrix}. \quad (3)$$

There exists a nondegenerate eigenspace and a unique dark state for the Hamiltonian $\mathcal{H}_R$, which is given by

$$|d_2(t)\rangle \propto (|\Omega_\mu|^2 - |\Omega_p|^2)|\phi_1\rangle + \Omega_p^2|\phi_4\rangle - \sqrt{2}\Omega_\mu\Omega_p|\phi_3\rangle. \quad (4)$$

Expressing the relative strength of the two Rabi frequencies Ω_p, Ω_μ as $\tan\theta = |\Omega_p|/|\Omega_\mu|$ and keeping their phases nonvanishing, Eq. (4) after normalization is rewritten as

$$\begin{aligned}
|d_2(t)\rangle = \mathcal{N}^{-1}[&(\cos^2\theta - \sin^2\theta)|\phi_1\rangle + \sin^2\theta e^{i2\phi_p}|\phi_4\rangle\\
&- \sqrt{2}\sin\theta\cos\theta e^{-i(\phi_\mu - \phi_p)}|\phi_3\rangle], \quad (5)
\end{aligned}$$

where

$$\cos\theta = \frac{|\Omega_\mu|}{\sqrt{|\Omega_\mu|^2 + |\Omega_p|^2}},$$

$$\sin\theta = \frac{|\Omega_p|}{\sqrt{|\Omega_\mu|^2 + |\Omega_p|^2}},$$

and

$$\mathcal{N} = \sqrt{\cos^4\theta + 2\sin^4\theta}.$$

Equation (5) has a similar form to the dark state firstly studied by Møller *et al.* [35], where a time-dependent relative phase $\phi_r(t) \equiv \phi_\mu - \phi_p$ is found to be relevant for acquisition of geometric phases, except that Eq. (5) contains an additional exponential factor $e^{i2\phi_p}$ for $|\phi_4\rangle$. It implies that by setting $\phi_p = 0$ or $\phi_p = \pi/2$, the two-atom system will transfer to the antisymmetric superposition state $|EPR\rangle_{as} = (|\phi_1\rangle - |\phi_4\rangle)/\sqrt{2}$ or the symmetric superposition state $|EPR\rangle_s = (|\phi_1\rangle + |\phi_4\rangle)/\sqrt{2}$ by adiabatically following the dark state with θ changing from 0 to $\pi/2$ (see later discussion for detail). This is numerically confirmed by examining the probability for detecting the two-atomic states $|EPR\rangle_{s,as}$ after the applied STIRAP pulse sequence [see Fig. 1(b)], which is a sinusoidal function of ϕ_p exhibiting wavelike interference fringes, as shown in Fig. 2. The coexistence of the phase factors 1, $e^{-i\phi_r}$ and $e^{i2\phi_p}$ in the superposition coefficients for

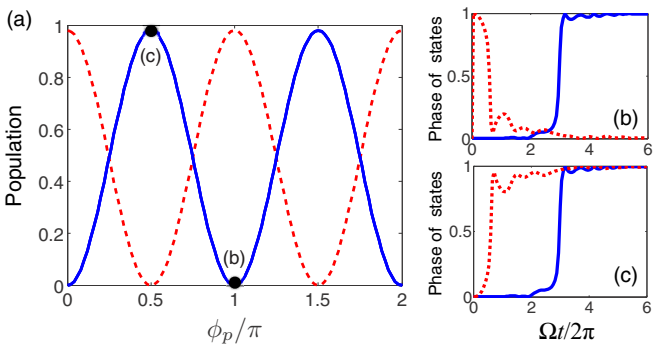

FIG. 2. (a) ϕ_p-dependent wavelike interference fringes in the probabilities of $|EPR\rangle_s$ (solid blue) and $|EPR\rangle_{as}$ (dashed red). (b, c) Numerically calculated time dependencies of the phases (divided by π) of the states $|\phi_1\rangle$ (solid blue) and $|\phi_4\rangle$ (dashed red) for $\phi_p = 0$ and $\phi_p = \pi/2$, respectively. The two-atom system is initially in the state $|\phi_1\rangle$ and adiabatically evolves along $|d_2(t)\rangle$. The Rabi frequencies are modeled by sine-function pulses $\Omega_p(t) = \Omega\sin(\frac{\pi}{2\tau}t)e^{i\phi_p}$, $\Omega_\mu(t) = \Omega|\cos(\frac{\pi}{2\tau}t)|$ with $0 \leqslant t \leqslant \tau$. We fix units of $\Omega = 1$, and set $\Omega\tau/2\pi = 6$, $V_{23}/\Omega = 1.1$, and $V_{33}/\Omega = 0.9$.

the three components $|\phi_1\rangle$, $|\phi_3\rangle$, and $|\phi_4\rangle$, respectively, can significantly modify the geometric phases acquired during adiabatic evolution assisted by phase control and can find special use for construction of quantum logic gates.

The level configuration [as in Fig. 1(a)] including a single Rydberg state suffers froman irreversible spontaneous decay since the optically excited intermediate state $|2\rangle$ has a short lifetime, therefore adiabatic manipulation of the (unstable) dark state becomes not experimentally feasible (see Sec. V for further discussion). To avoid the defect, we then consider atoms with two ground hyperfine states $|0\rangle$ and $|1\rangle$ and two Rydberg state $|2\rangle$ and $|3\rangle$; see Fig. 1(c). The atomic transition $|1\rangle \leftrightarrow |2\rangle$ is resonantly excited by a single-photon field Ω_p, and the transition $|2\rangle \leftrightarrow |3\rangle$ is driven by a microwave field Ω_μ. The auxiliary level $|0\rangle$ is introduced as a qubit information for the later discussed gate protocols. While both atoms are excited to the Rydberg states, two relevant interparticle interactions are involved, i.e., the van der Waals (vdW) interaction V_{22} (V_{33}) between the states $|2\rangle$ ($|3\rangle$) and the exchange dipole-dipole interaction (DDI) V_{23} between an atom in $|2\rangle$ and another in $|3\rangle$. When including the Rydberg-Rydberg interaction, the two-atom Hamiltonian governing the temporal evolution of the compound system takes the form

$$\begin{aligned}\mathcal{H}'_R = {} & \mathcal{H}_1 \otimes \mathcal{I}_2 + \mathcal{I}_1 \otimes \mathcal{H}_2 + V_{33}|3\rangle_1|3\rangle_{22}\langle 3|_1\langle 3| \\ & + V_{22}|2\rangle_1|2\rangle_{22}\langle 2|_1\langle 2| + V_{23}(|2\rangle_1|3\rangle_{22}\langle 3|_1\langle 2| \\ & + |3\rangle_1|2\rangle_{22}\langle 2|_1\langle 3|). \end{aligned} \tag{6}$$

If the two atoms only weakly interact with each other while they are in the state $|2\rangle$ (e.g., due to a dispersive Förster process) such that the vdW shift V_{22} becomes negligible comparing with other Rydberg interaction energies V_{33}, V_{23}, i.e., $V_{22} \ll V_{23}, V_{33}$, then the Hamiltonian $\mathcal{H}'_R$ with $V_{22} \to 0$ has one dark state, which is exactly given by Eq. (5). The interatomic DDI V_{23} does not shift the zero eigenenergy and change the form of the dark state. Therefore, the single-Rydberg-level effects with respect to $|d_2\rangle$ hold true for the multiple-Rydberg-level model as long as the adiabatic condition is well guaranteed, and adiabatic control of the dark state becomes more feasible for long radiative lifetime of the Rydberg levels.

In another parameter regime where the interaction between the Rydberg states $|3\rangle$ is sufficiently weak comparing with the vdW shift V_{22} and the DDI strength V_{23}, i.e., $V_{33} \ll V_{22}, V_{23}$, by setting $V_{33} = 0$ we again find a dark state for $\mathcal{H}'_R$, but with a different form,

$$\begin{aligned}|d'_2(t)\rangle = {} & \cos^2\theta e^{i2\phi_r}|\phi_1\rangle + \sin^2\theta|\phi_6\rangle \\ & - \sqrt{2}\sin\theta\cos\theta e^{i\phi_r}|\phi_3\rangle, \end{aligned} \tag{7}$$

which can be exactly expressed as the direct product of the dark states for the single-atom Hamiltonian $\mathcal{H}_i$ ($i = 1,2$), i.e., $|d'_2(t)\rangle = |d_1(t)\rangle_1 \otimes |d_1(t)\rangle_2$, with

$$|d_1(t)\rangle_i = \cos\theta e^{i\phi_r}|1\rangle_i - \sin\theta|3\rangle_i. \tag{8}$$

In this case, the relative phase ϕ_r is the only degree of freedom for phase modulation during the system's adiabatic evolution along $|d'_2(t)\rangle$.

If we further assume that $V_{22} = V_{33} = 0$ but with $V_{23} \neq 0$, the zero-energy eigenstate for the two-atom Hamiltonian $\mathcal{H}'_R$ can then be written as the superposition of the degenerated dark states $|d_2(t)\rangle$ and $|d'_2(t)\rangle$. A finite Rydberg interaction strength V_{22} or V_{33} between the states $|2\rangle$ or $|3\rangle$ results in the removal of the degeneracy, which cannot occur with only the DDI due to the missing component $|\phi_5\rangle$.

Suppose that the Hamiltonian $\mathcal{H}'_R(t)$ is time dependent through the set of parameters $\mathbf{R}(t) = (\theta(t), \phi_p(t), \phi_r(t))$ and the interacting two-atom system is initially in the ground eigenstate $|g[\mathbf{R}(0)]\rangle$ of the instantaneous $\mathcal{H}'_R(t = 0)$. If $\mathbf{R}(t) = (\theta(t), \phi_p(t), \phi_r(t))$ is modulated under the condition

$$|\langle e(t)|\frac{d\mathcal{H}'_R}{dt}|g(t)\rangle| \ll |E_e - E_g|^2$$

such that the Hamiltonian is adiabatically changed along a closed curve $\boldsymbol{C}$ in the parameter space [i.e., $\mathbf{R}(T) = \mathbf{R}(0)$], where $|e\rangle$ is any one of the instantaneous excited state, then the system will keep in the ground state and acquire a purely geometric phase φ_g in additional to the usual dynamical phase φ_d:

$$|g[\mathbf{R}(T)]\rangle = \exp\{i[\varphi_g(T) + \varphi_d(T)]\}|g[\mathbf{R}(0)]\rangle, \tag{9}$$

where

$$\varphi_g = i\oint_{\boldsymbol{C}} d\mathbf{R} \cdot \langle g[\mathbf{R}(t)]|\nabla_{\mathbf{R}}|g[\mathbf{R}(t)]\rangle \tag{10}$$

and

$$\varphi_d(T) = -\int_0^T E_d[\mathbf{R}(t)]\, dt, \tag{11}$$

which vanishes for a dark state $|g(t)\rangle = |d[\mathbf{R}(t)]\rangle$ with zero eigenenergy $E_g = 0$.

III. SCHEMES FOR IMPLEMENTING CONTROLLED-Z GATES VIA ADIABATIC PASSAGE

We encode qubit information on the ground state $|1\rangle$ and the auxiliary level $|0\rangle$ that is uncoupled from any pulse sequences of the control field. Thus, the computational basis states are given by $\{|0\rangle_1|0\rangle_2, |0\rangle_1|1\rangle_2, |1\rangle_1|0\rangle_2, |1\rangle_1|1\rangle_2\}$. The controlled-Z gate is implemented by applying a counterintuitive pulse sequence and by modulating the phases of the control fields.

A. Scheme 1

Here we have a geometric phase gate with the phases of the Rabi frequencies varying in step (i.e., $\phi_r = \text{const}$). It has been realized that the dark states (5) and (8) under adiabatic evolution can acquire the geometric phases $\varphi_2 = 2\int \sin^2\theta\cos^2\theta(\cos^4\theta + 2\sin^4\theta)^{-1}\, d\phi_r$ and $\varphi_1 = \int \sin^2\theta\, d\phi_r$, respectively, for a nonvanishing and time-dependent relative phase $\phi_r(t)$ [35]. In contrast, we find that the two-atom dark state (5) can acquire a Berry phase even though the relative phase is kept invariant.

Suppose the two-atom system is initially in $|d_2(0)\rangle = |1\rangle_1|1\rangle_2$ (i.e., $\cos\theta = 1$) and the phases of the driving fields are $\phi_p(0) = 0$, $\phi_\mu(0) = 0$ without loss of generality. The time-dependent amplitudes of the Rabi frequencies are chosen as ($0 \leqslant t \leqslant 2\tau$)

$$|\Omega_p(t)| = \Omega\sin\left(\frac{\pi}{2\tau}t\right), \quad |\Omega_\mu(t)| = \Omega\left|\cos\left(\frac{\pi}{2\tau}t\right)\right|, \tag{12}$$

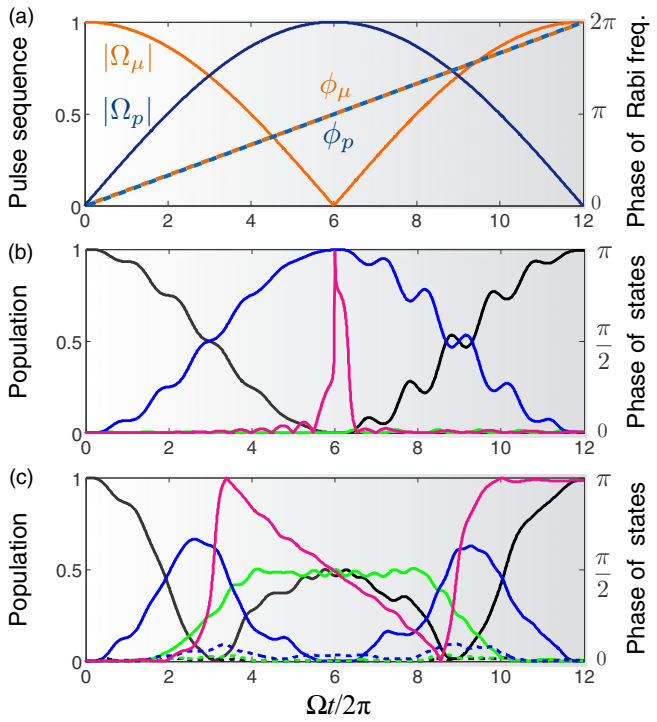

FIG. 3. (a) The amplitudes $|\Omega_p(t)|$, $|\Omega_\mu(t)|$ and phases ϕ_p, ϕ_μ of Rabi frequencies as a function of rescaled time. (b) Time-dependent population of the states $|0\rangle_1|1\rangle_2$ ($|1\rangle_1|0\rangle_2$) (black), $|0\rangle_1|3\rangle_2$ ($|3\rangle_1|0\rangle_2$) (blue), and $|0\rangle_1|2\rangle_2$ ($|2\rangle|0\rangle_2$) (green), and the phase of state $|0\rangle_1|1\rangle_2$ ($|1\rangle_1|0\rangle_2$) (magenta) for the system initially in $|d_1(0)\rangle$. (c) Time-dependent population of the states $|1\rangle_1|1\rangle_2$ (solid black), $|\phi_2\rangle$ (dash black), $|\phi_3\rangle$ (solid blue), $|\phi_4\rangle$ (solid green), $|\phi_5\rangle$ (dash green), and $|\phi_6\rangle$ (dash blue), and the phase of state $|1\rangle_1|1\rangle_2$ (magenta) for the system initially in $|d_2(0)\rangle$. We fix units of $\Omega = 1$, and set $\Omega\tau/2\pi = 6$, $V_{23}/\Omega = 1.1$, and $V_{33}/\Omega = 0.9$.

which corresponds to $\theta(t)$ varying from 0 to $\pi/2$ and the corresponding reverse process. The phases $\phi_{p,\mu}(t)$ are synchronized with each other in real time and have a simply linear time dependence $\phi_{p,\mu}(t) = \pi t/\tau$. Therefore, the system makes a cyclic evolution with starting point and ending point $\theta = 0$; see the temporal evolution of the probability amplitudes and the phases of the relevant states as shown in Fig. 3. The geometric phase φ_2' (i.e., the Berry phase) accumulated during the adiabatic process can be calculated by using the standard formula (10). Since ϕ_r remains zero at any time, the relevant parameter space reduces to $\mathbf{R}(t) = (\theta(t),\phi_p(t))$. Thus, we have

$$\begin{aligned}\varphi_2' &= -\oint_C \frac{2\sin^4\theta}{\cos^4\theta + 2\sin^4\theta} d\phi_p \\ &= -\oint_C \frac{4\sin^4\theta}{\cos^4\theta + 2\sin^4\theta} d\theta \end{aligned} \tag{13}$$

for $d\phi_p(t)/d\theta(t) = 2$ taken in our example. Apart from that, while the system is initially in the state $|0\rangle_1|0\rangle_2$, $|0\rangle_1|1\rangle_2$ or $|1\rangle_1|0\rangle_2$, no geometric phases can be acquired during the cyclic evolution. The sudden increase of the phases of $|0\rangle_1|1\rangle_2$ ($|1\rangle_1|0\rangle_2$) around $t = \tau$ is due to imperfect state transfer and is automatically eliminated at the end of the pulse sequence. Thus, we have successfully implemented a controlled phase gate based on the conditionally geometric phase shift:

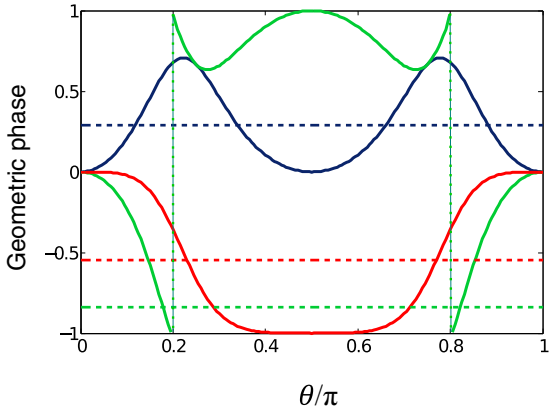

FIG. 4. The acquired geometric phases φ_2, φ_2', and φ_2'' versus θ. The system in the initial state $|d_2(0)\rangle = |1\rangle_1|1\rangle_2$ is adiabatically taken to the superposition state with a given θ followed by sweeping the phase of the controlled fields: ϕ_p, ϕ_μ: $0 \to \pi$ (red), $\phi_p = 0$, ϕ_μ: $0 \to \pi$ (blue) and ϕ_p: $0 \to \pi$, $\phi_\mu = 0$ (green), respectively. The amplitudes of the applied pulse sequence and other parameters are as in Fig. 3.

$$\begin{aligned}&|0\rangle_1|0\rangle_2 \to |0\rangle_1|0\rangle_2, \quad |0\rangle_1|1\rangle_2 \to |0\rangle_1|1\rangle_2, \\ &|1\rangle_1|0\rangle_2 \to |1\rangle_1|0\rangle_2, \quad |1\rangle_1|1\rangle_2 \to e^{i\varphi_2'}|1\rangle_1|1\rangle_2. \end{aligned} \tag{14}$$

Since we have guaranteed $\phi_r = \text{const}$ during the adiabatic evolution, the required solid angle for obtaining the geometric phase φ_2' is induced by the concurrency control of ϕ_p and ϕ_μ, where an additional reference oscillator should be included. While for the system initially being in the two-atom dark state $|d_2'(t)\rangle$ under the condition $V_{33} \ll V_{22,}V_{23}$, no geometric phases can be acquired since ϕ_r is invariant.

However, if ϕ_r becomes time variant, note that the phases of the Rabi frequencies may be modulated in two fashions, leading to differently geometric phase shift for the state $|d_2\rangle$. First, $\phi_p = \text{const}$ and $\phi_r(t) = \phi_\mu(t) - \phi_p$ is time dependent via $\phi_\mu(t)$. In this case, the geometric phase acquired is exactly given by φ_2. While for the other case where $\phi_\mu = \text{const}$ and $\phi_r(t) = \phi_\mu - \phi_p(t)$ is determined by $\phi_p(t)$, the geometric phase acquired is then alternatively given by

$$\begin{aligned}\varphi_2'' &= -\oint_C \frac{2\sin^2\theta}{\cos^4\theta + 2\sin^4\theta} d\phi_p \\ &= -\oint_C \frac{4\sin^2\theta}{\cos^4\theta + 2\sin^4\theta} d\theta. \end{aligned} \tag{15}$$

Thus, we find three different ways of phase control for geometrically manipulating the interacting two-atom system. A comparison of the acquired geometric phases for the three cases is shown in Fig. 4, from which one can easily read φ_2, φ_2', and φ_2'' by $4\theta_m\overline{f(\theta)}$, with θ_m and $\overline{f(\theta)}$ being the given θ with respect to the preset dark state $d_2(\theta_m,\phi_p,\phi_\mu)$ and the θ average of the curves on the plots (indicated by dash lines for scheme 1), respectively.

B. Scheme 2

Here we have a gate based on the non-Berry adiabatic phase arising from staircase phase control. The operation procedure is generally divided into two steps during the time interval $0 \leqslant t \leqslant 2\tau$, in which the time-dependent amplitudes of the Rabi frequencies again vary according to Eq. (12), and the phases of the driving fields follow

$$\phi_p(t) = \text{const}, \quad \phi_r(t) = \frac{\pi}{2}\Theta(t-\tau), \tag{16}$$

with $\Theta(x)$ being the unit step function. Note that the relative phase is changed only at the end of the first half of the pulse sequence ($t = \tau$) without the limit of adiabaticity, and the system Hamiltonian is not changed along a closed curve in the parameter space $\mathbf{R}(t) = (\theta(t), \phi_r(t))$. Therefore, it is fundamentally different from the geometric operation (leading to the Berry phase) proposed by Møller *et al.* [35], where the relative phase should be adiabatically modulated when the applied pulses overlap, and the initial and the final Hamiltonian of the evolutional system should remain the same [i.e., $\mathbf{R}(2\tau) = \mathbf{R}(0)$]. The idea of realizing a phase gate through adiabatic manipulation of the dark state with staircase phase control was studied in ion traps [41].

In the first step ($0 \leqslant t \leqslant \tau$), the phase factors ϕ_p, ϕ_μ are set to be equal so that $\phi_r = 0$, e.g., $\phi_p = \phi_\mu = 0$ for simplicity. θ is adiabatically increased from 0 to $\pi/2$ by adjusting the relative intensity of the coupling fields as in Eq. (12). For $V_{22} \ll V_{23}, V_{33}$, the temporal evolution of the basis states will follow the dark states [Eqs. (5) and (8)] throughout the procedure, leading to the transformations

$$\begin{aligned} &|0\rangle_1|0\rangle_2 \to |0\rangle_1|0\rangle_2, \quad |0\rangle_1|1\rangle_2 \to -|0\rangle_1|3\rangle_2, \\ &|1\rangle_1|0\rangle_2 \to -|3\rangle_1|0\rangle_2, \quad |1\rangle_1|1\rangle_2 \to \frac{1}{\sqrt{2}}(-|\phi_1\rangle + |\phi_4\rangle). \end{aligned} \tag{17}$$

In the second step ($\tau \leqslant t \leqslant 2\tau$), θ is tuned adiabatically from $\pi/2$ back to 0 but with $\phi_p = 0$ and $\phi_\mu = \pi/2$ (i.e., $\phi_r = \pi/2$), which gives rise to

$$\begin{aligned} &|0\rangle_1|0\rangle_2 \to |0\rangle_1|0\rangle_2, \quad -|0\rangle_1|3\rangle_2 \to e^{i\pi/2}|0\rangle_1|1\rangle_2, \\ &-|3\rangle_1|0\rangle_2 \to e^{i\pi/2}|1\rangle_1|0\rangle_2, \quad \frac{1}{\sqrt{2}}(-|\phi_1\rangle + |\phi_4\rangle) \to |1\rangle_1|1\rangle_2. \end{aligned} \tag{18}$$

Since the two processes are highly adiabatic, the population of the basis states return to the initial state after the counterintuitive pulse sequence. It is interesting to see that the basis states $|0\rangle_1|1\rangle_2$ and $|1\rangle_1|0\rangle_2$ finally acquire an additional phase factor $e^{i\varphi_{ng}}$ with $\varphi_{ng} = \pi/2$, which does not exist for $|0\rangle_1|0\rangle_2$ and $|1\rangle_1|1\rangle_2$ (see Fig. 5). Because the dark states are the eigenstates of $\mathcal{H}_i$ ($i = 1,2$) with zero eigenvalues, φ_{ng} has no dynamic origin. On the other hand, here the Hamiltonian is not required to make a cyclic evolution in the parameter space as for the accumulation of the adiabatic Berry phase.

Finally, by applying single-qubit operations $|1\rangle_{1,2} \to e^{i\pi/2}|1\rangle_{1,2}$ to both atoms, we recover the familiar controlled-Z gate

$$\begin{aligned} &|0\rangle_1|0\rangle_2 \to |0\rangle_1|0\rangle_2, \quad |0\rangle_1|1\rangle_2 \to |0\rangle_1|1\rangle_2, \\ &|1\rangle_1|0\rangle_2 \to |1\rangle_1|0\rangle_2, \quad |1\rangle_1|1\rangle_2 \to -|1\rangle_1|1\rangle_2, \end{aligned} \tag{19}$$

which can be easily transformed to a controlled-NOT gate by using two additional $\pi/2$ pulses rotating the target qubit around the y axis in the opposite directions. Note that for $V_{33} \ll V_{22}, V_{23}$, repeating the operation procedure above will lead to the transformation for the basis states: $|0\rangle_1|1\rangle_2 \to e^{i\pi/2}|0\rangle_1|1\rangle_2$, $|1\rangle_1|0\rangle_2 \to e^{i\pi/2}|1\rangle_1|0\rangle_2$ and $e^{i\pi}|1\rangle_1|1\rangle_2$, which is impossible to become a universal binary gate under any local operations.

From a comparison between the two schemes we can see that the non-Berry phase gate via the staircase phase control is built on a completely different mechanism in contrast to the normal dynamical and geometric phase gates: the qubit system does not undergo any dynamical phase shift since it works in the zero-energy eigenspace; the Hamiltonian is not changed along a closed curve in the parameter space; precise adiabatic modulation of the phases of the driving fields and adiabatic control of the population transfer at the same time is unnecessary, and thus, the errors in obtaining the required

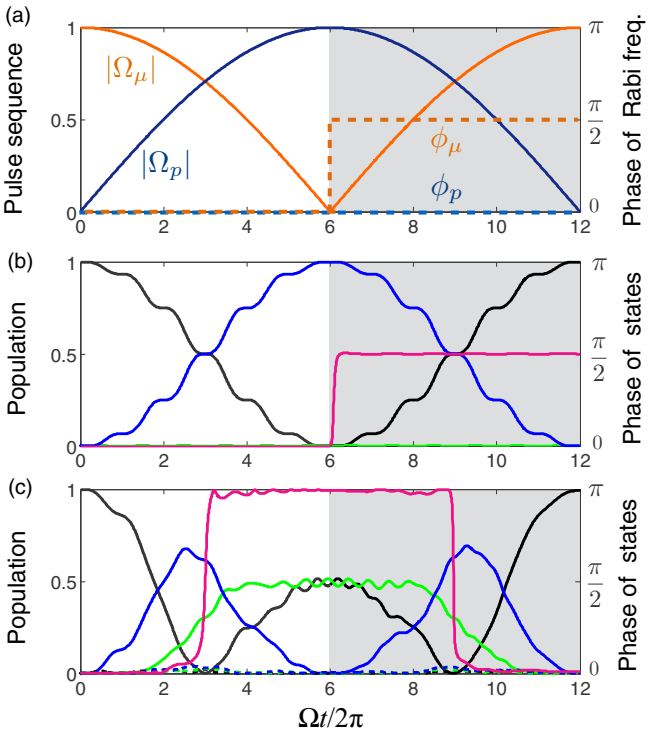

FIG. 5. (a) The amplitudes $|\Omega_p(t)|$, $|\Omega_\mu(t)|$ and phases ϕ_p, ϕ_μ of Rabi frequencies as a function of rescaled time. Without loss of generality, we set $\phi_{p,\mu}(0) = 0$. (b) Time dependence of the population of states $|0\rangle_1|1\rangle_2$ ($|1\rangle_1|0\rangle_2$) (black), $|0\rangle_1|3\rangle_2$ ($|3\rangle_1|0\rangle_2$) (blue), and $|0\rangle_1|2\rangle_2$ ($|2\rangle|0\rangle_2$) (green), and the phase of state $|0\rangle_1|1\rangle_2$ ($|1\rangle_1|0\rangle_2$) (magenta) for the system initially in $|d_1(0)\rangle$. (c) Time dependence of the population of states $|1\rangle_1|1\rangle_2$ (solid black), $|\phi_2\rangle$ (dash black), $|\phi_3\rangle$ (solid blue), $|\phi_4\rangle$ (solid green), $|\phi_5\rangle$ (dash green), and $|\phi_6\rangle$ (dash blue), and the phase of state $|1\rangle_1|1\rangle_2$ (magenta) for the system initially in $|d_2(0)\rangle$. Other parameters as same in Fig. 3.

geometric solid angle are avoided and the operation procedure is simplified.

IV. PHYSICAL REALIZATION: ASYMMETRIC RYDBERG COUPLING

In the context of Rydberg experiments, the strongly asymmetric coupling condition $V_{22} \ll V_{23}, V_{33}$ can be found, for example, by mapping the Rydberg states to $|2 = 40p_{3/2}, m = 1/2\rangle$ and $|3 = 41s_{1/2}, m = 1/2\rangle$ of rubidium atoms separated at an interatomic distance R of several micrometers. In this case, the blockade interaction between the states $|2\rangle$ and $|3\rangle$ is an exchange process of resonant dipole nature ($\sim n^4/R^3$ with n being the principal quantum number), where the zero-interaction angle can be avoided either by using a spatial light modulator to create the preset trap pattern or by applying a weak external magnetic field ($B = 10^{-7}$ T) to couple the atomic Zeeman states of different magnetic quantum numbers. The anisotropic interaction between states $|2\rangle$ and isotropic interaction between states $|3\rangle$ are both induced by the Förster process, where the two-atomic interaction potential can transit from the dipole-dipole to the van der Waals limit ($\sim n^{11}/R^6$), depending on the interatomic distance [42]. It is therefore possible to restrict our consideration to the asymmetric coupling regime, which represents the dominant interaction mechanism at the atomic separation of interest. For $R = 3\,\mu$m, the interaction strengths V_{23} and V_{22} can, respectively, vary from 5 to 20 MHz, and from 0.02 to 0.1 MHz by adjusting the angle between the dipoles, and the interaction strength V_{33} approximates $2\pi \times 3.7$ MHz [43].

On the other hand, the excitation of Rydberg p-states from ground s-states in a single-photon transition has recently become feasible due to the availability of ultraviolet laser sources, which results in much larger Rabi frequency Ω (scaling as $\Omega \sim n^{-3/2}$) compared to a three-photon excitation process [44]. In addition, the optical excitation of a Rydberg state followed by a microwave-driven coupling between two neighboring Rydberg levels has been experimentally demonstrated as well, where the Rabi frequency of the Rydberg-Rydberg transition can reach several tens of MHz by increasing the intensity of the microwave field [45]. Thus, it becomes very promising to implement the proposed schemes with asymmetric Rydberg-Rydberg interaction by integrating the current experimental techniques [46].

To evaluate the performance of the controlled-Z gate, we use the fidelity $F = [\mathrm{Tr}\sqrt{\sqrt{\rho_{tar}}\rho(2\tau)\sqrt{\rho_{tar}}}]^2$ to measure the desired output ρ_{tar} given an input of all the logical states $|\psi_0\rangle = \frac{1}{2}(|0\rangle_1|0\rangle_2 + |0\rangle_1|1\rangle_2 + |1\rangle_1|0\rangle_2 + |1\rangle_1|1\rangle_2)$, where $\rho_{tar} = |\psi_{tar}\rangle\langle\psi_{tar}|$ with $|\psi_{tar}\rangle$ being the target state obtained through an ideal gate operation $|\psi_{tar}\rangle = U_{CZ}|\psi_0\rangle$, and $\rho(2\tau)$ is the actual output state in the logical space produced in the presence of the error sources, such as nonadiabatic transitions, docoherence induced by atomic spontaneous emission, and atomic motion. In Fig. 6, we have shown the fidelity of the controlled-Z gate [Eqs. (14) and (19)] under the condition of asymmetric Rydberg coupling $V_{22} \ll V_{23}, V_{33}$ in the coherent regime. Considering the dynamically perturbative effect of V_{22} (i.e. $V_{22}\tau \ll 1$), the fidelity reaches its optimum at $V_{33} = 0.7$, $V_{23} = 1$ and $V_{33} = 0.9$, $V_{23} = 1$ for gates based on the Berry and the non-Berry adiabatic phase, respectively,

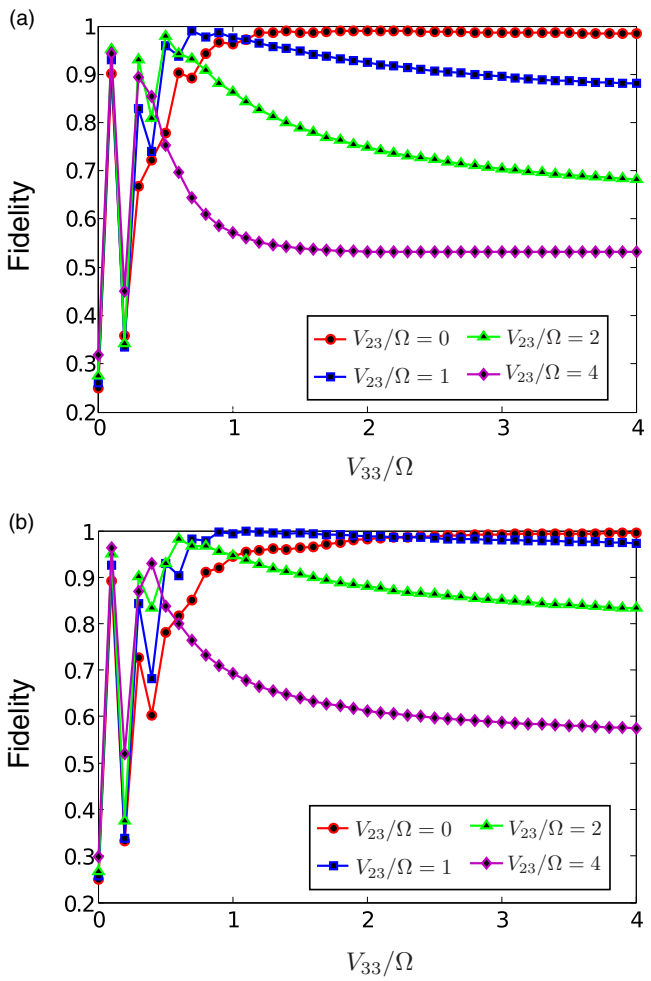

FIG. 6. Fidelities of gates based on Berry phase (a) and non-Berry adiabatic phase (b) vs the energy shift V_{33}/Ω of the collective Rydberg states $|3\rangle_1|3\rangle_2$ for the DDI strength $V_{23}/\Omega = 0, 1, 2, 4$ (from top to bottom) and $V_{22}/\Omega = 0.005$. Other parameters are as in Fig. 3.

where the interaction strengths V_{23}, V_{33} are of comparable magnitude with the maximum of the Rabi frequencies Ω, corresponding to the intermediate coupling regime $V_{23}, V_{33} \sim \Omega$. Further increasing V_{23} or V_{33} will lead to reduction of the gate fidelity (due to nonadiabatic transfer towards the nonzero-energy eigenstates); however, note that the non-Berry operation is more robust against the variation of the Rydberg interactions compared with the geometric Berry operation. For the special situation where $V_{22} \simeq 0$ and $V_{23} = 0$, available for a cascaded level configuration involving a single Rydberg state (see later discussion), the condition for a high-fidelity gate performance is simply $V_{33} > 2\Omega$, which lies in the regime of Rydberg blockade. In this case, the optimal implementation of the Berry-phase-based controlled-Z gate requires slightly weaker V_{33} than that for the non-Berry adiabatic operation, but again, the latter exhibits its robustness as V_{33} increases.

For small V_{33}, the temporal evolution of the system is no longer adiabatically confined in the state $|d_2(t)\rangle$ and the effect of the other dark component $|d_2'(t)\rangle$ should be considered. In this case, the nonadiabatic transition to the doubly excited state $|3\rangle_1|3\rangle_2$ accompanied with interatomic interaction will

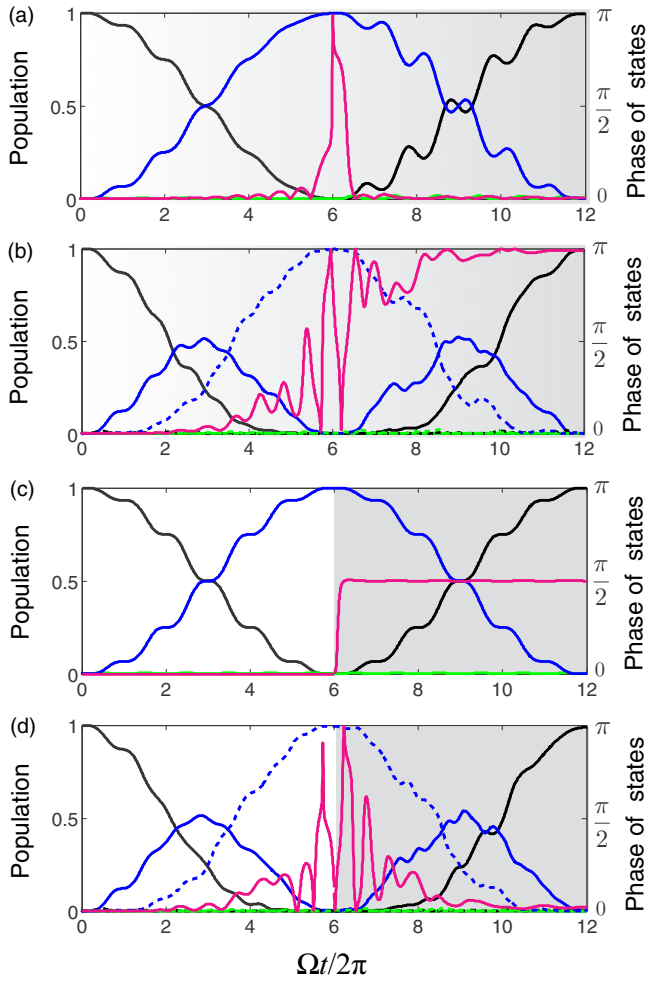

FIG. 7. Time dependence of the state populations during the gate operations based on Berry phase [(a), (b)] and non-Berry adiabatic phase [(c), (d)] with $(V_{22}, V_{23}, V_{33})/\Omega = (1, 1.5, 0.1)$. The color scheme and other parameters are as in Fig. 3.

introduce a dynamical phase, which may be constructive for implementing the controlled-Z gate as well. To gain the insight, we have repeated the procedures for generating the Berry and the non-Berry phases as before under the condition of $V_{33} \ll V_{22}, V_{23}$. If $V_{33} = 0$, the system strictly evolves along the dark state $|d_2'(t)\rangle$, where the phase difference ϕ_r of the control fields becomes the only relevant phase factor for the modulation process. For the operation to obtain Berry phases, the system acquires no geometric phase during the cyclic evolution since ϕ_r is kept invariant [see Figs. 7(a)–7(b)]. Alternatively, for the operation to obtain non-Berry adiabatic phases, the rise of ϕ_r at $t = \tau$ introduces phase factors $e^{i2\phi_r} = e^{i\pi}$ and $e^{i\phi_r} = e^{i\pi/2}$ to the basis states $|1\rangle_1|1\rangle_2$ and $|1\rangle_1|0\rangle_2$ (or $|0\rangle_1|1\rangle_2$), respectively, which are irrelevant to a binary gate. But for a finite V_{33}, the instantaneous ground state of $\mathcal{H}_R'$ evolves from the bare $|1\rangle_1|1\rangle_2$ state into a "dressed" state with some admixture of $|3\rangle_1|3\rangle_2$, which additionally supplements a dynamical phase $\varphi_d \approx \int \sin^4\theta V_{33}\, dt$ to $|1\rangle_1|1\rangle_2$ [see Figs. 7(c)–7(d)]. Therefore, the implementation of a controlled-Z gate via the completely dynamical control is still available for $\varphi_d = \pi$ for both cases and is sensitive to the fluctuation of Rydberg interactions nevertheless.

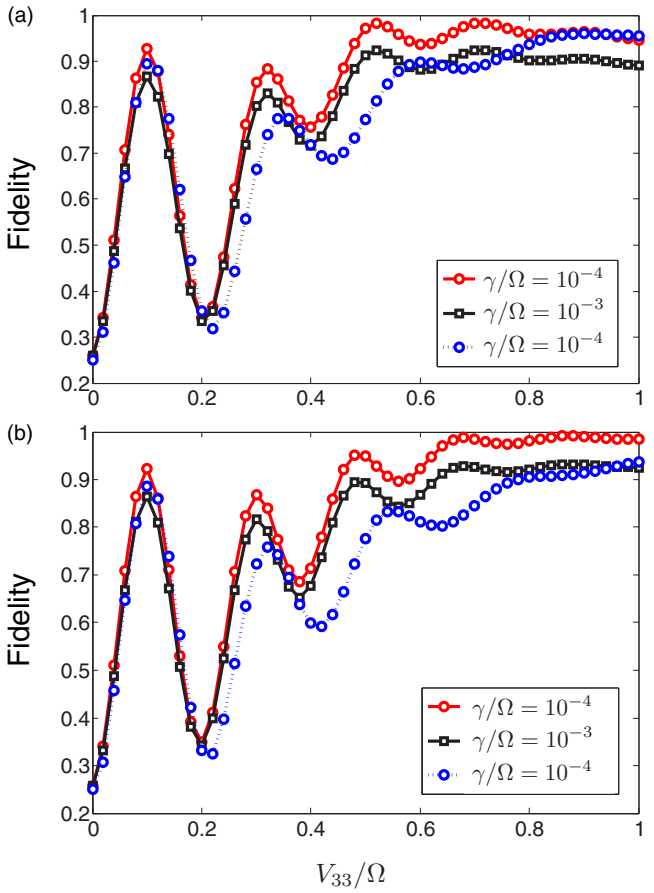

FIG. 8. Fidelities of the gates based on Berry phase (a) and non-Berry adiabatic phase (b) for different atomic spontaneous emission rates as functions of the Rydberg interaction V_{33} for $(V_{22}, V_{23})/\Omega = (0.005, 1)$ (solid) and $V_{22} = V_{23} = 0$ (dash). We here set $\gamma_2 = \gamma_3 = \gamma$.

V. THE EFFECT OF SPONTANEOUS EMISSION AND INTERATOMIC FORCE

The two atoms excited to Rydberg states are subjected to decoherence due to atomic spontaneous emission and interatomic force. The dissipative dynamics can be calculated by the Lindblad master equation for the density operator ρ of the two-atom system,

$$\dot{\rho}(t) = -i[\mathcal{H}_R', \rho(t)] + \sum_{i=1}^{2}\sum_{k=1}^{2} \mathcal{L}[A_{i,k}]\rho(t), \qquad (20)$$

where $\mathcal{L}[A_{i,k}]\rho = A_{i,k}\rho A_{i,k}^\dagger - \frac{1}{2}\{A_{i,k}^\dagger A_{i,k}, \rho\}$, $A_{i,1} = \sqrt{\gamma_2}|1\rangle_{ii}\langle 2|$ and $A_{i,2} = \sqrt{\gamma_3}|2\rangle_{ii}\langle 3|$ with γ_2 and γ_3 being the spontaneous decay rates for the transition channels $|2\rangle_i \to |1\rangle_i$ and $|3\rangle_i \to |2\rangle_i$ respectively. In Fig. 8 we show overlap (fidelity) between the realistic density matrix $\rho(2\tau)$ at the end of the pulse sequences from Eq. (20) and the ideal result ρ_{tar} (for $\gamma_2 = \gamma_3 = 0$), for the system initially in $|\psi_0\rangle$. Since the lifetime of the Rydberg states $|2\rangle$ ($|3\rangle$) with principal quantum number $n = 40$ or 41 is around $60\,\mu s$, thus the decay rates are taken as $\gamma_2 = \gamma_3 = 10^{-4}\Omega$, $10^{-3}\Omega$, corresponding to the peak Rabi frequency $\Omega/2\pi = 20$ MHz, 2 MHz, respectively. For the former case, the fidelities of the gates relying on the Berry phase and non-Berry adiabatic phase are 0.983 and

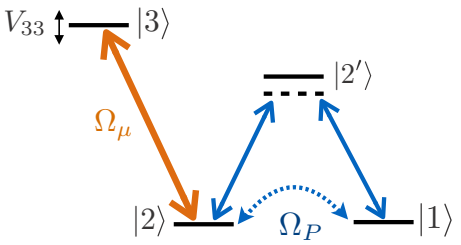

FIG. 9. Level configuration. Two hyperfine ground states $|1\rangle$, $|2\rangle$ are coupled via the Raman process with the effective Rabi frequency Ω_p. The Rydberg state $|3\rangle$ is excited via a single-photon transition of the Rabi frequency Ω_μ.

0.992, respectively; while for the latter case, fidelity of better than 0.92 is still achievable for both schemes. On the other hand, the interatomic force (induced by double excitation of Rydberg states) during the gate operation can couple the internal degree of freedom to the externally atomic motion. Its perturbative effect on the gate fidelity can be estimated by $\sim \frac{3\lambda_0 V_{33}}{R\omega_0}(1-e^{-i\omega_0\tau})$ to the first order, with ω_0 the trapping frequency and λ_0 the wavelength of trapping light [7]. Thus, one can enlarge the Rabi frequency Ω to reduce the gate duration τ or alternatively use an optical lattice (instead of an optical tweezer trap) with higher trapping frequency to trap the atoms such that the motional effect can be reasonably ignored.

As mentioned before, the controlled-Z gate can be implemented as well with the atomic level scheme involving only a single Rydberg state. In this case, the microwave control becomes unnecessary. However, for the usual Rydberg EIT configuration (i.e., a cascaded three-level system), the populated intermediate state $|2\rangle$ (such as $6p_{1/2}$ for Rb and $7p_{1/2}$ for Cs atoms) is an excited state with strong spontaneous emission rate, which will irreversibly deteriorate the coherent population transfer and then the gate fidelity [7,35]. However, the obstacle can be overcome by using the single-photon excitation scheme for the ground-Rydberg transition and by mapping $|1\rangle$ and $|2\rangle$ to the atomic hyperfine states, which can couple to each other via two-photon Raman processes (see Fig. 9). Therefore, the fidelity can be further improved by selecting a Rydberg state with larger principal quantum number and longer lifetime. For example, in a 300 K environment, the Cs Rydberg states $|90p\rangle$, $|95p\rangle$ have the lifetimes 361 μs and 406 μs, respectively [9]. Moreover, double excitation of Rydberg states is avoided, and thus the effect of the interatomic force that may entangle their motional degree of freedom can be neglected.

VI. CONCLUSION

In conclusion, we have shown that the Rydberg-Rydberg interaction between two highly excited atoms can be exploited for implementing a reliable controlled-Z gate via adiabatic passage and tailored phase modulation. The developed addressing schemes drive the system Hamiltonian to change in a cyclic or a noncyclic manner, giving rise to a Berry phase or a non-Berry adiabatic phase for implementation of conditional phase gates. In the former case, the geometric phase is acquired through concurrent control of the phases of the driving fields and can be alternatively obtained via modulation of the relative phase in two different ways, while for the latter the requirement of adiabatic phase control becomes unnecessary, and therefore the experimental complexity can be significantly released. We also pointed out that the implementation of the schemes with multilevel atomic configuration involving a unique Rydberg state might be more promising for experimental demonstration. We note that our adiabatic Rydberg gates may not replace the conventional approaches with fast dynamical control; however, the merits of the adiabatic technique itself and the addressing schemes of phase modulation found here will provide perspectives for adiabatic manipulation of interacting Rydberg systems.

ACKNOWLEDGMENTS

This work was supported by the National Natural Science Foundation of China under Grants No. 11374054, No. 11534002, No. 11674060, No. 11575045, No. 11774058, and No. 11405031, and the Natural Science Foundation of Fujian Province under Grant No. 2017J01401.

[1] M. Saffman, T. G. Walker, and K. Mølmer, Rev. Mod. Phys. **82**, 2313 (2010).
[2] A. Browaeys, D. Barredo, and T. Lahaye, J. Phys. B: At. Mol. Opt. Phys. **49**, 152001 (2016).
[3] M. Cozzini, T. Calarco, A. Recati, and P. Zoller, Opt. Commun. **264**, 375 (2006).
[4] E. Brion, L. H. Pedersen, and K. Mølmer, J. Phys. B: At. Mol. Opt. Phys. **40**, S159 (2007).
[5] M. Müller, I. Lesanovsky, H. Weimer, H. P. Büchler, and P. Zoller, Phys. Rev. Lett. **102**, 170502 (2009).
[6] H.-Z. Wu, Z.-B. Yang, and S.-B. Zheng, Phys. Rev. A **82**, 034307 (2010).
[7] D. D. Bhaktavatsala Rao and K. Mølmer, Phys. Rev. A **89**, 030301(R) (2014).
[8] T. Keating, R. L. Cook, A. M. Hankin, Y.-Y. Jau, G. W. Biedermann, and I. H. Deutsch, Phys. Rev. A **91**, 012337 (2015).
[9] I. I. Beterov, M. Saffman, E. A. Yakshina, D. B. Tretyakov, V. M. Entin, S. Bergamini, E. A. Kuznetsova, and I. I. Ryabtsev, Phys. Rev. A **94**, 062307 (2016).
[10] J. Zeiher, P. Schauß, S. Hild, T. Macrì, I. Bloch, and C. Gross, Phys. Rev. X **5**, 031015 (2015).
[11] E. Brion, L. H. Pedersen, M. Saffman, and K. Mølmer, Phys. Rev. Lett. **100**, 110506 (2008).
[12] A. Chen, Opt. Express **19**, 2037 (2011).
[13] J. Sanders, R. van Bijnen, E. Vredenbregt, and S. Kokkelmans, Phys. Rev. Lett. **112**, 163001 (2014).
[14] D. Petrosyan, M. Saffman, and K. Mølmer, J. Phys. B: At. Mol. Opt. Phys. **49**, 094004 (2016).
[15] Y. Han, B. He, K. Heshami, C. Z. Li, and C. Simon, Phys. Rev. A **81**, 052311 (2010).
[16] B. Zhao, M. Müller, K. Hammerer, and P. Zoller, Phys. Rev. A **81**, 052329 (2010).

[17] E. Brion, F. Carlier, V. M. Akulin, and K. Mølmer, Phys. Rev. A **85**, 042324 (2012).
[18] N. Solmeyer, X. Li, and Q. Quraishi, Phys. Rev. A **93**, 042301 (2016).
[19] D. Jaksch, J. I. Cirac, P. Zoller, S. L. Rolston, R. Côté, and M. D. Lukin, Phys. Rev. Lett. **85**, 2208 (2000).
[20] M. D. Lukin, M. Fleischhauer, R. Cote, L. M. Duan, D. Jaksch, J. I. Cirac, and P. Zoller, Phys. Rev. Lett. **87**, 037901 (2001).
[21] L. Isenhower, E. Urban, X. L. Zhang, A. T. Gill, T. Henage, T. A. Johnson, T. G. Walker, and M. Saffman, Phys. Rev. Lett. **104**, 010503 (2010).
[22] X. L. Zhang, A. T. Gill, L. Isenhower, T. G. Walker, and M. Saffman, Phys. Rev. A **85**, 042310 (2012).
[23] M. M. Müller, M. Murphy, S. Montangero, T. Calarco, P. Grangier, and A. Browaeys, Phys. Rev. A **89**, 032334 (2014).
[24] K. M. Maller, M. T. Lichtman, T. Xia, Y. Sun, M. J. Piotrowicz, A. W. Carr, L. Isenhower, and M. Saffman, Phys. Rev. A **92**, 022336 (2015).
[25] S.-L. Su, Y. Gao, E. Liang, and S. Zhang, Phys. Rev. A **95**, 022319 (2017).
[26] D. Petrosyan and K. Mølmer, Phys. Rev. Lett. **113**, 123003 (2014).
[27] D. Barredo, S. Ravets, H. Labuhn, L. Béguin, A. Vernier, F. Nogrette, T. Lahaye, and A. Browaeys, Phys. Rev. Lett. **112**, 183002 (2014).
[28] Y. Zeng, P. Xu, X. D. He, Y. Y. Liu, M. Liu, J. Wang, D. J. Papoular, G. V. Shlyapnikov, and M. S. Zhan, arXiv:1702.00349.
[29] N. V. Vitanov, A. A. Rangelov, B. W. Shore, and K. Bergmann, Rev. Mod. Phys. **89**, 015006 (2017).
[30] I. I. Beterov, D. B. Tretyakov, V. M. Entin, E. A. Yakshina, I. I. Ryabtsev, C. MacCormick, and S. Bergamini, Phys. Rev. A **84**, 023413 (2011).
[31] D. Yan, C. L. Cui, M. Zhang, and J. H. Wu, Phys. Rev. A **84**, 043405 (2011),.
[32] J. Qian, J. Zhai, L. Zhang, and W. Zhang, Phys. Rev. A **91**, 013411 (2015).
[33] X.-D. Tian, Y.-M. Liu, C.-L. Cui, and J.-H. Wu, Phys. Rev. A **92**, 063411 (2015).
[34] D. Petrosyan, D. D. Bhaktavatsala Rao, and K. Mølmer, Phys. Rev. A **91**, 043402 (2015).
[35] D. Møller, L. B. Madsen, and K. Mølmer, Phys. Rev. Lett. **100**, 170504 (2008).
[36] M. H. Goerz, E. J. Halperin, J. M. Aytac, C. P. Koch, and K. B. Whaley, Phys. Rev. A **90**, 032329 (2014).
[37] I. I. Beterov, M. Saffman, E. A. Yakshina, V. P. Zhukov, D. B. Tretyakov, V. M. Entin, I. I. Ryabtsev, C. W. Mansell, C. MacCormick, S. Bergamini *et al.*, Phys. Rev. A **88**, 010303 (2013).
[38] Y.-C. Zheng and T. A. Brun, Phys. Rev. A **86**, 032323 (2012).
[39] S.-B. Zheng, Phys. Rev. A **91**, 052117 (2015).
[40] S.-B. Zheng, C. P. Yang, and F. Nori, Phys. Rev. A **93**, 032313 (2016).
[41] S.-B. Zheng, Phys. Rev. Lett. **95**, 080502 (2005).
[42] M. Saffman and K. Mølmer, Phys. Rev. A **78**, 012336 (2008).
[43] M. Saffman and K. Mølmer, Phys. Rev. Lett. **102**, 240502 (2009).
[44] A. M. Hankin, Y.-Y. Jau, L. P. Parazzoli, C. W. Chou, D. J. Armstrong, A. J. Landahl, and G. W. Biedermann, Phys. Rev. A **89**, 033416 (2014).
[45] D. Maxwell, D. J. Szwer, D. Paredes-Barato, H. Busche, J. D. Pritchard, A. Gauguet, K. J. Weatherill, M. P. A. Jones, and C. S. Adams, Phys. Rev. Lett. **110**, 103001 (2013).
[46] D. Barredo, H. Labuhn, S. Ravets, T. Lahaye, A. Browaeys, and C. S. Adams, Phys. Rev. Lett. **114**, 113002 (2015).